Available online at www.sciencedirect.com
ScienceDirect
Bioorganic & Medicinal Chemistry 16 (2008) 5695–5703
Bioorganic & Medicinal Chemistry

SAR and QSAR study on 2-aminothiazole derivatives, modulators of transcriptional repression in Huntington's disease

Samantha Leone,[a] Cesare Mutti,[b] Aleksey Kazantsev,[c] Mattia Sturlese,[d] Stefano Moro,[d] Elena Cattaneo,[e] Dorotea Rigamonti[b,*] and Alessandro Contini[a,*]

[a]*Istituto di Chimica Organica "Alessandro Marchesini", Facoltà di Farmacia, Università degli Studi di Milano, Via Venezian 21, 20133 Milano, Italy*
[b]*Dialectica S.r.l., c/o Nerviano Medical Sciences, V.le Pasteur 10, 20014 Nerviano MI, Italy*
[c]*MassGeneral Institute for Neurodegenerative Diseases, Massachusetts General Hospital, Building 114-3300, 16th Street, Charlestown, MA 02129-4404, USA*
[d]*Molecular Modeling Section, Dipartimento di Scienze Farmaceutiche, Università di Padova, Via Marzolo 5, Padova, Italy*
[e]*Dipartimento di Scienze Farmacologiche, Università degli Studi di Milano, Via Balzaretti 9, 20133 Milano, Italy*

Received 15 December 2007; revised 14 March 2008; accepted 25 March 2008
Available online 30 March 2008

Abstract—REST/NRSF is a multifunctional transcription factor that represses or silences many neuron-specific genes in both neural and non-neural cells by recruitment to its cognate RE1/NRSE regulatory sites. An increase in RE1/NRSE genomic binding is found in Huntington's disease (HD), resulting in the repression of REST/NRSF regulated gene transcription, among which BDNF, thus representing one of the possible detrimental effectors in HD. Three 2-aminothiazole derivatives were recently identified as potent modulators of the RE1/NRSE silencing activity through a cell-based gene reporter assay. In this study, the structure–activity relationships (SAR) of a library of commercially available 2-aminoisothiazoles diversely substituted at the amino group or at position 4 has been evaluated. A quantitative structure–activity relationship analysis performed using the Phase strategy yielded highly predictive 3D-QSAR pharmacophore model for in silico drug screening.

1. Introduction

Huntington's disease (HD) is a dominantly inherited neurodegenerative disorder for which there is no effective treatment, although a number of underlying pathogenic mechanisms have been identified and indicate that more than one therapeutic target should be investigated.[1–3] The protein responsible for HD is the huntingtin protein, which has been shown by a number of studies to be neuroprotective under normal conditions,[4] although mutations can make it toxic and deprive it of its beneficial activities.[4,5] We here concentrate on the identification of small molecules capable of interfering with one of the critical molecular dysfunctions caused by huntingtin mutations.

The repressor element 1/neuron-restrictive silencer element (NRSE/RE1) is a silencer element that is present upstream of more than 1300 neuronal genes,[6–9] including brain-derived neurotrophic factor (BDNF), a neurotrophin that is essential for the correct functioning of the neurons that die in HD.[10,11] Under normal conditions, its activity is regulated by the silencing transcription factor/neuron-restrictive silencer factor (REST/NRSF), a repressor factor whose binding stimulates the silencer and leads to reduced neuronal gene transcription.[12] We have previously reported that the transcription of BDNF and many other NRSE-controlled neuronal genes is severely reduced in HD due to a pathological translocation of REST/NRSF into the nucleus, and the aberrant activation of RE1/NRSE.[13–15] This means that compounds capable of inhibiting RE1/NRSE transcriptional activity in HD cells should contribute towards restoring the lost transcription, thus possibly

Keywords: 2-Aminothiazoles; Huntington's disease; Structure–activity relationship; 3D-QSAR; Pharmacophore.
* Corresponding authors. Tel.: +39 0331 581971; fax: +39 0331 581235 (D.R.); tel.: +39 02 50314480; fax: +39 02 50314476 (A.C.); e-mail addresses: drigamonti.dialectica@nervianoms.com; alessandro.contini@unimi.it

0968-0896/$ - see front matter © 2008 Elsevier Ltd. All rights reserved.
doi:10.1016/j.bmc.2008.03.067

improving the underlying neuropathology[16]; furthermore, their impact may also extend to other diseases involving the RE1/NRSE-REST/NRSF pathway, such as ischemic stress,[17,18] Down's syndrome[19] and some medulloblastomas.[20]

We have recently identified three potent analogues as being capable of influencing RE1/NRSE transcriptional activity by showing that (a) these increased the activity of a reporter construct placed downstream of a RE1/NRSE silencer; (b) these increased endogenous BDNF gene transcription in a dose-dependent manner and at nanomolar concentrations; and (c) these activities could be detected in cells bearing the mutant protein, thus suggesting the ability of the compounds to interfere with the underlying pathogenic mechanism.[21] We now report the structure–activity relationships (SAR) of a library of commercially available 2-aminoisothiazoles variously substituted in *region 1* and *region 2* as shown in Figure 1. We also made a quantitative structure–activity relationship (QSAR) analysis using a 3D-QSAR strategy, in which a reasonable 3D-pharmacophore model was developed on the basis of Phase methodology.[22,23]

2. Results and discussion

2.1. Library selection

Starting from the hit compound **2** (Fig. 1), a similarity search was performed using the Ligand-Info system,[24] which includes a number of publicly available small molecule databases (ChemBank, ChemPDB, KEGG, NCI, AKos GMBH, Asinex Ltd and TimTec) covering more than one million compounds. The clustering and search algorithms implemented in Ligand-Info are based on a two-dimensional structure similarity technique in which molecular structures are represented by modified hashed fingerprints, and the similarity is expressed as a modified Tanimoto coefficient (MTC).[25] All the molecules with an MTC value of >0.72 were selected in order to generate a focused library of 2-aminothiazoles with differences in *regions 1* and *2*, as shown in Figure 1.

The selected library consisted of 84 unique and commercially available molecules, including the three compounds identified in Ref. 21, and was acquired for biochemical testing; however, for the sake of clarity, the discussion below will be limited to a selection of 45 structures covering all the investigated chemical features. The full list of compounds and their measured activities are provided as Supporting Information.

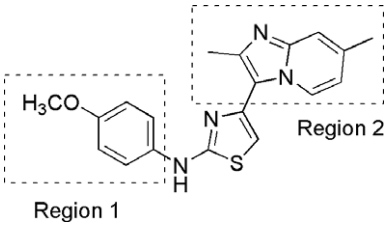

Figure 1. Selected regions of interest for SAR evaluation.

2.2. Cell-based reporter assay for monitoring RE1/NRSE silencing activity

The DiaNRSE^{Luc8} cell system is able to reveal the activity of tested compounds on the RE1/NRSE transcriptional element. These cells have been genetically and chemically previously validated for the correct responsiveness of the RE1/NRSE silencer.[21] We here used the DiaNRSE^{Luc8} cell system to monitor the activities of a series of 81 analogues of the identified compounds **2**, **18** and **19**, which were also retested for comparison. Table 1 shows the fold-increase in luciferase activity normalised by the number of cells in the treated and untreated samples. All the molecules were tested at a concentration of 50 nM and the assay was performed 72 h after exposure to the compounds. The histone deacetylase (HDAC) inhibitor trichostatin A (TSA), a known broad transcriptional activator, was included in each experiment as a positive control.

2.3. SAR study

Table 1 summarises the activities of a representative series of 2-aminothiazoles, expressed as fold-increase (*FI*) in reporter gene expression. The influence of the *region 1* or *2* variations on the observed activity is described below.

2.3.1. *Region 1* substitutions. One *conditio sine qua non* for the ability of 2-aminothiazoles to reduce RE1/NRSE silencer activity is the substitution at the amino group by an aromatic function: it can be seen that the allylic derivative **E5** and the unsubstituted compound **F5** are totally inactive, and the presence of a carbonyl spacer group also reduces activity. This is particularly evident when comparing the active compound **F1** ($FI = 1.90 \pm 0.35$) with its closely analogous but totally inactive derivative **A5** ($FI = 0.94 \pm 0.13$), and confirmed by the fact that the other amido derivatives **D3**, **D7**, **G3** and **D6** are inactive. Other aromatic groups associated with a loss of activity are 2-methylenfurane (see **1B1**), 4-methylpyridin-2yl (see **B2**) and benzene (see **1D1**). The replacement of the carbonyl spacer in compounds **D3** and **D6** by a methylene group (respectively, giving rise to **1D3** and **1B1**) does not lead to any change in the measured activity.

Compound **C6**, which differs from **1D3** insofar as *region 2* bears a 2,7-dimethylimidazo[1,2-*a*]pyridine instead of a 2-methylimidazo[1,2-*a*]pyridine, shows very modest activity ($FI = 1.30 \pm 0.26$). As will be discussed later, this substitution does not lead to any considerable change in the activity of the other investigated compounds, and so the activity of **C6** should not be considered relevant.

In terms of aromatic ring substitutions, none of the *ortho*-substituted (**D5** and **1A7**), *meta*-substituted (**B2**, **1B4** and **G5**), or *di*-(**E4**, **A4** and **B7**) or *tri*-substituted compounds (**C7** and **D4**) shows any marked activity, whereas the *para*-substitution clearly and positively affects activity, as demonstrated by comparing the measured activities of the close analogues **O** and **D5** (1.88 ± 0.37 vs 0.94 ± 0.02) or **G4** and **1A7** (2.29 ± 0.76 vs 0.97 ± 0.08).

Table 1. Compounds selected for SAR investigation and their measured biological activity[a]

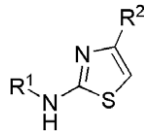

Entry	R^1	R^2	Activity (*FI*)
2	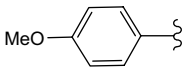	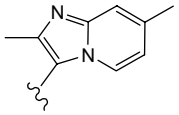	2.19 ± 0.90
18	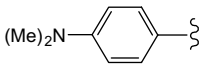	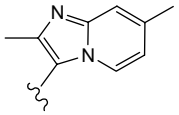	2.55 ± 0.74
19	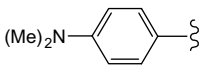	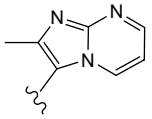	3.34 ± 0.99
A	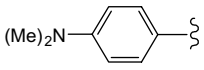	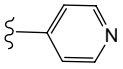	1.13 ± 0.03
D	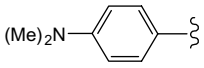	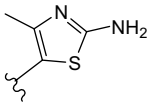	1.23 ± 0.63
E	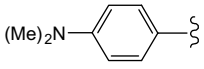	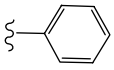	1.30 ± 0.60
1B6	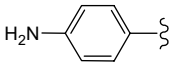	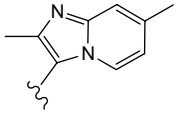	1.14 ± 0.19
C4	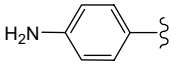	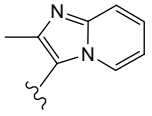	1.28 ± 0.30
N	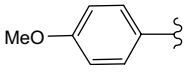	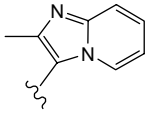	2.00 ± 0.55
E3	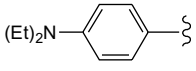	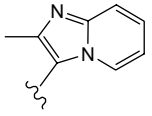	1.09 ± 0.15
1D2	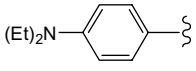	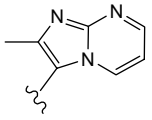	1.16 ± 0.37
G4	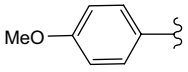	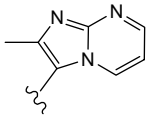	2.29 ± 0.76
E4	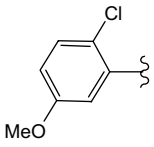	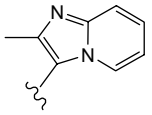	1.09 ± 0.30

(*continued on next page*)

Table 1 (*continued*)

Entry	R^1	R^2	Activity (*FI*)
A4	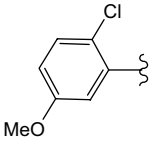	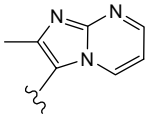	0.74 ± 0.15
1D4	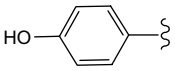	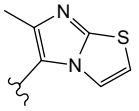	0.95 ± 0.25
1B5	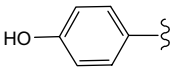	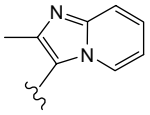	1.02 ± 0.15
B7	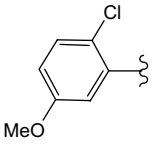	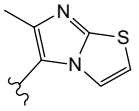	0.91 ± 0.09
1C2	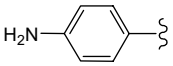	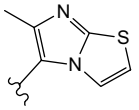	1.14 ± 0.11
1A6	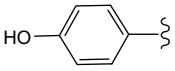	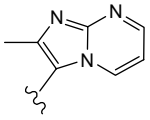	0.89 ± 0.13
1C3	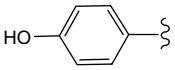	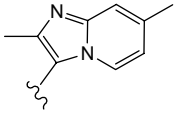	1.08 ± 0.13
D3	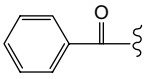	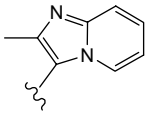	1.09 ± 0.27
D7	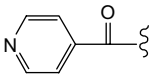	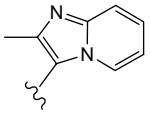	1.00 ± 0.10
G3	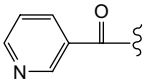	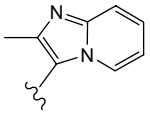	0.98 ± 0.03
1D3	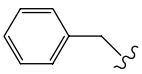	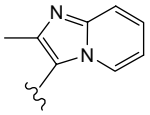	0.97 ± 0.20
F5	H-	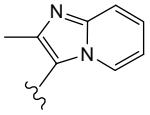	0.87 ± 0.06
E5		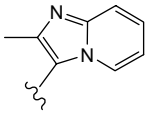	0.91 ± 0.08
D6	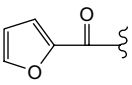	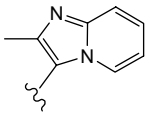	0.94 ± 0.11
1B1	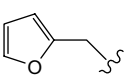	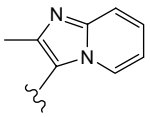	1.01 ± 0.20

Table 1 (*continued*)

Entry	R^1	R^2	Activity (*FI*)
B2	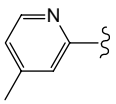	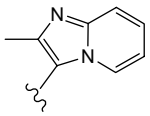	0.98 ± 0.12
1D1	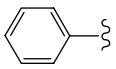	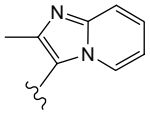	1.01 ± 0.13
F6	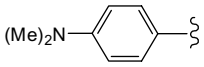	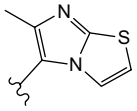	1.80 ± 0.42
1B4	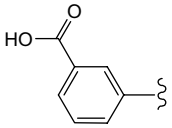	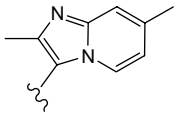	1.14 ± 0.13
C5	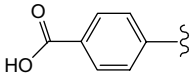	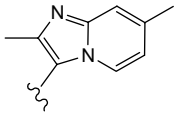	1.12 ± 0.15
G5	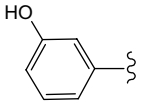	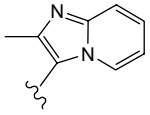	1.04 ± 0.13
O	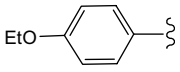	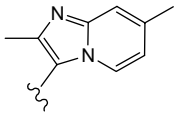	1.88 ± 0.37
D5	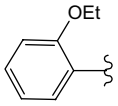	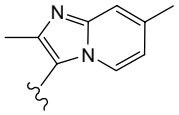	0.94 ± 0.02
1A7	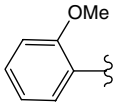	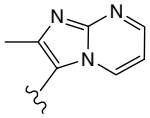	0.97 ± 0.08
C7	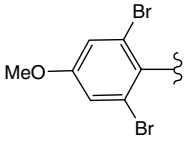	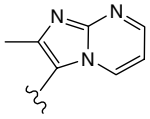	1.03 ± 0.16
D4	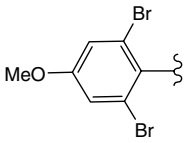	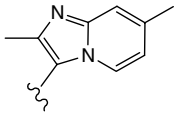	1.07 ± 0.18
F1	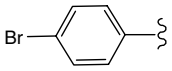	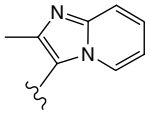	1.90 ± 0.35
A5	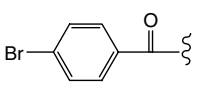	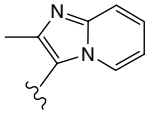	0.94 ± 0.13
C6	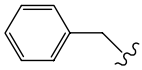	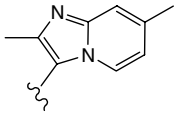	1.30 ± 0.26

(*continued on next page*)

Table 1 (*continued*)

Entry	R^1	R^2	Activity (*FI*)
1B2	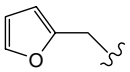	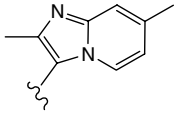	0.99 ± 0.02
D2	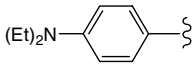	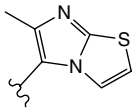	1.04 ± 0.21
E1	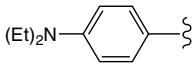	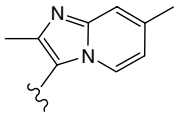	1.06 ± 0.23

[a] The biological activity is expressed as fold-increase (FI) in luciferase activity in treated versus untreated samples. Experiments were performed 72 h after exposure to 50 nM of the indicated compounds.

Regarding the chemical features of the *para*-substituent, analysis of the biochemical results obtained for the two sets of close analogues, respectively, bearing an amine, dimethylamine or diethylamine in the phenyl *para*-position (**1C2**, **F6** and **D2**, and **1B6**, **18** and **E1**) show that the dimethylamino derivatives **F6** and **18** are the most active (*FI* values of, respectively, 1.80 ± 0.42 and 2.55 ± 0.74), whereas the amino- (**1C2, 1B6**) and diethylamino-derivatives (**D2**, **E1**) are almost completely inactive. Similarly, if we consider the compounds bearing a hydroxy (**1D4**, **1B5**, **1A6** and **1C3**), methoxy (**2**, **N** and **G4**) or ethoxy group (**O**) in the phenyl *para*-position, the first group is more active than the last, but the methoxy-substituted compounds are the most active; this is further highlighted by the *FI* values of the close analogues **1B5** and **N** (1.02 ± 0.15 and 2.00 ± 0.55), **1A6** and **G4** (0.89 ± 0.13 and 2.29 ± 0.76), or **1C3**, **O** and **2** (1.08 ± 0.13, 1.88 ± 0.37 and 2.19 ± 0.90). On the basis of the above, it can be deduced that the *para*-substituent should be a hydrogen-bond acceptor substituted by a moderately encumbering aliphatic group but, surprisingly, compound **F1**, which bears a bromine atom as the *para*-substituent, was also active.

Other *para*-substituents such as the carboxyl- (**C5**) or nitro-groups (**E6**) do not lead to any activity.

It can therefore be said that a substituent in the *para*-position of the aromatic ring in *region 1* with good lyophilicity and moderate steric encumbrance positively affects the ability of 2-aminothiazoles to increase reporter activity in DiaNRSE^{LUC8} cells.

2.3.2. *Region 2* substitutions. The loss of in vitro activity observed when the 2-methylimidazo[1,2,-*a*]pyridine or 2-methylimidazo[1,2,-*a*]pyrimidine derivatives **18** and **19** were changed to the aromatic monocycle substituted derivatives **A**, **D** and **E** (R^2 = pyridine, 2-amino-4-methylthiazole and benzene, respectively) suggests that activity requires a bicyclic heterocycle in *region 2*. However, the chemical nature of the bicyclic moiety may vary considerably because, for example, the presence of a methyl group in the 2-methylimidazo[1,2-*a*]pyridine position 7 is scarcely relevant, as in the case of compounds **1B6** and **C4** or compounds **2** and **N**, in which comparable RE1/NSRE modulating capabilities were detected (1.14 ± 0.19 for **1B6** and 1.28 ± 0.30 for **C4**, and 2.19 ± 0.90 for **2** and 2.00 ± 0.55 for **N**). Moreover, similar activity profiles are maintained when the carbon atom in 2-methylimidazo[1,2-*a*]pyridine position 8 is replaced by a nitrogen, thus obtaining the 2-methylimidazo[1,2-*a*]pyrimidine derivatives, as is shown by the close analogues **E3** and **1D2** (1.09 ± 0.15 and 1.16 ± 0.37), **E4** and **A4** (1.09 ± 0.30 and 0.74 ± 0.15) or **N** and **G4** (2.00 ± 0.55 and 2.29 ± 0.76). However, it should be noted that, when the C7 methyl group is replaced by a hydrogen and the C8 with a nitrogen, there is a slight variation in RE1/NSRE modulating ability, as observed in the case of compounds **18** and **19** (2.55 ± 0.74 and 3.34 ± 0.99). Finally, the activity profile is also maintained when the 2-methylimidazo[1,2-*a*]pyridine or the 2-methylimidazo[1,2-*a*]pyrimidine is replaced by the 6-methylimidazo[2,1-*b*]thiazole moiety, as shown by comparing the potent compounds **18** and **19** with **F6** (1.8 ± 0.42), which shows only a slight decrease in activity, or by comparing the inactive compounds **1D4**, **B7** and **1C2** (0.95 ± 0.25,) with their thiazole analogues **1B5**, **E4** and **C4**.

2.4. 3D-QSAR study

In order to investigate the quantitative relationships between the activity of 2-aminothiazole derivatives and the nature of the R^1 and R^2 substituents, and derive a predictive model that will be useful in future screening experiments, the $[\log(FI)] \times 100$ values were analysed using a 3D-QSAR strategy. Discovering three-dimensional pharmacophores that can explain the activity of a series of ligands is one of the most significant contributions of computational chemistry to drug discovery, and Phase is one of the most recently developed pharmacophore modelling tools.[17] Phase has a hypothesis-generating step based on a grid-based 3D-QSAR method in which the grid positions of the atoms in the molecules superimposed on the hypotheses are correlated with their activities using a partial-least-squares (PLS) fitting.

As we used Phase methodology to create a reasonable 3D-pharmacophore model with the aim of further rationalising the observed SAR, we selected 42 2-aminothiazoles as a training set for 3D-pharmacophore elucidation. For each 2-aminothiazole analogue, a group of suitable pharmacophore sites (features) were assigned from which to derive a set of suitable pharmacophores. For this step, we chose a $[\log(FI)] \times 100$ value of >18 as the threshold for defining an 'active' compound because it generally corresponds to a result in which the measured fold-increase (*FI*) in the luciferase activity of the investigated compound minus the experimental standard deviation is more than the *FI* value plus the standard deviation of the untreated control. By analysing the ability of all the possible pharmacophore site combinations to classify active and inactive compounds correctly, we finally identified a 5-feature (H-acceptor, H-donor, hydrophobic, and two aromatic features) model as the best pharmacophoric descriptor of the training set (see Fig. 2).

Interestingly, all the selected pharmacophore features have previously been described as being crucial for the rationalisation of the observed SARs of this new class of 2-aminothiazoles. Once all the ligands were overlaid with our best Phase hypothesis, an atom-based 3D-QSAR analysis was derived on the basis of standard Phase parameters. Table 2 shows all the statistical parameters derived using Phase methodology. The correlation coefficients are statistically acceptable ($r^2 = 0.84$ and $q^2 = 0.84$ with only three principal components, PCs), supporting the robustness of the statistical model. Moreover, the very high Pearson r (r_p) value also indicates a close correlation between the predicted and actual $[\log(FI)] \times 100$ values (r_p ranging from +1.0 (perfect correlation) to −1.0 (perfect anti-correlation)). The predicted and actual $[\log(FI)] \times 100$ values of the Phase model with the highest r^2 and q^2 are shown in Figure 3.

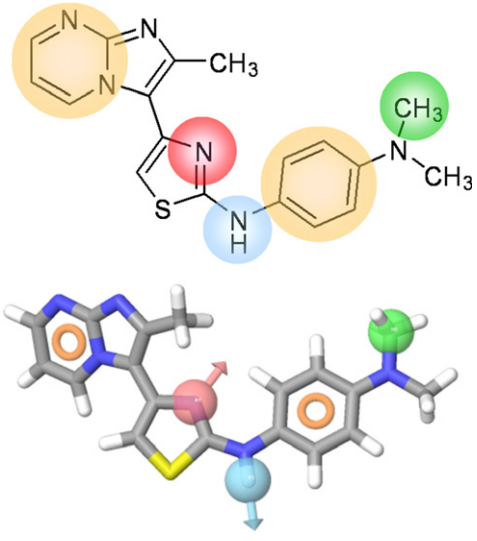

Figure 2. The best Phase hypothesis superimposed on the most active RE1/NRSE silencer modulator (compound **19**); green: hydrophobic aliphatic; orange: hydrophobic aromatic; red: H-bond acceptor; blue: H-bond donor.

Table 2. 3D-QSAR statistical parameters

Summary of PLS model statistic	
Training set	26
Test set	16
*PC*s	3
r^2	0.84
q^2	0.84
r_p	0.94
SD	6.39
RMSE	5.52

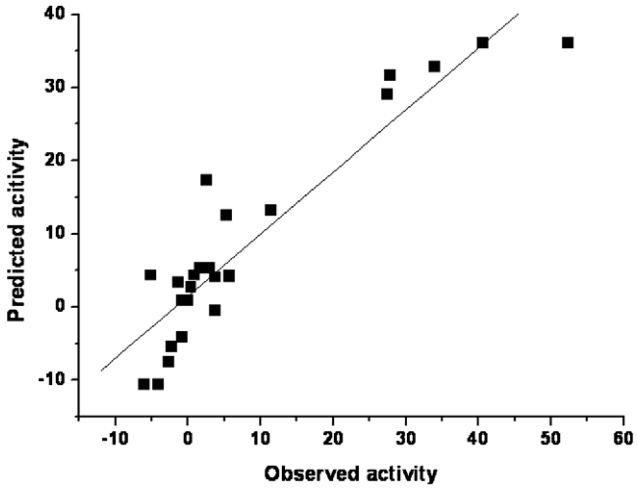

Figure 3. Predicted versus actual $[log(FI)] \times 100$ values for the Phase model with the highest r^2 and q^2.

The 3D-QSAR results can also be visualised using 3D plots of the crucial pharmacophore regions: the blue cubes refer to ligand regions in which the specific feature is important for high activity, whereas the red cubes suggest that the activity of the same ligand feature substitution is less. Figure 4 shows the 3D-QSAR results for the H (hydrophobic/non-polar), D (donor) and A (acceptor) and R (aromatic) features relating to the most active RE1/NRSE silencer modulator overlaid with the best Phase hypothesis (compound **19**).

3. Conclusion

The inhibition of RE1/NRSE transcriptional activity increases the transcription of neuronal genes (including the BDNF gene), which should be beneficial in human neurodegenerative diseases such as HD. Herein, we have reported the first SAR study of a series of 2-aminothiazoles that suppress RE1/NRSE silencing activity. The analysis, aimed at elucidating the effect on activity of the substituents in the amino group (*region 1*) and position 4 (*region 2*), show that the aromatic ring in *region 1* should be substituted in the *para*-position by a hydrophobic group with slight steric encumbrance, but H-bond acceptor capabilities are also desirable. At the same time, *region 2* should be characterised by an aromatic bicycle containing heteroatoms with H-bond acceptor capabilities. The 2-aminoisothiazole moiety and the methyl group in position 2 of the bicyclic

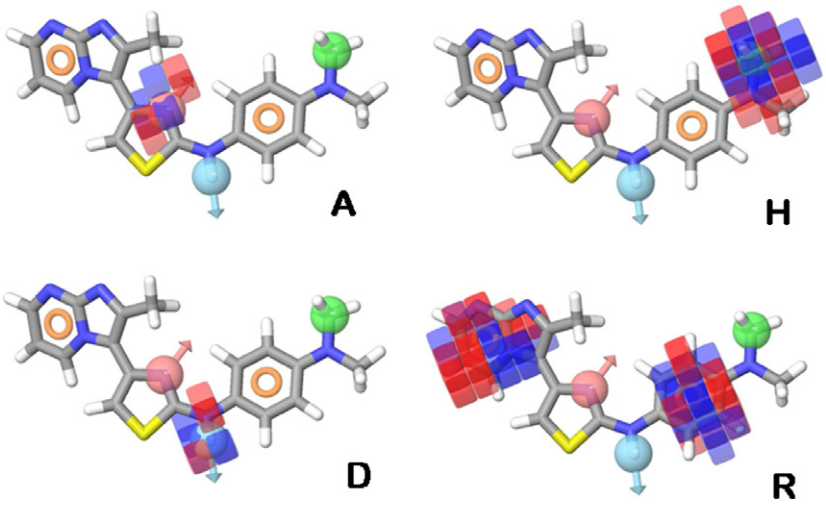

Figure 4. 3D-pharmacophore regions around compound **19**. The blue and red cubes refer to ligand regions in which a molecular substitution with a specific feature behaviour, respectively, increases or decreases binding affinity for the target. A = hydrogen-bond acceptor feature; D = hydrogen-bond donor feature; H = hydrophobic, non-polar feature; and R = aromatic feature.

heterocycle were kept constant in the series of evaluated compounds, and their role in determining the RE1/NRSE modulating activity will be the object of future studies. Although none of the screened molecules resulted more effective than the originally identified compounds, five new derivatives proved to be active. Thus, by disposing of a set of eight diversely substituted and active 2-aminothiazoles we developed a statistically robust 3D-pharmacophore model using Phase methodology. This model is capable of appropriately describing the variability of our internal test, and its good predictivity further support the observations based on the SAR analysis. Although we are aware about the local character of the 3D-QSAR model herein presented, we would like to emphasize that, at the moment, no other data-set are available and this is the first attempt to rationalize the observed activity of substituted 2-aminothiazoles. Reasonably, the predictivity shown by our model could be helpful for designing new strictly related derivatives while the 3D-pharmacophore model can be also used for the virtual screening of large databases with the aim of identifying new classes of RE1/NRSE silencer modulators.

4. Experimental

4.1. Chemicals

All the described compounds were obtained from ChemBridge Corp. (UK) and Asinex Ltd (Moscow, Russia), and were guaranteed by the resellers as being at least 95% pure. The lyophilised powder was dissolved in 100% DMSO (SIGMA, Milano, Italy) to a final concentration of 10 mM. The working solutions were prepared by diluting the stock solution 1:100 in DMSO to a concentration of 100 μM, and then stored at −20 °C until being thawed away from sources of light for a few minutes before the preparation of the testing solutions. The testing solutions were prepared by diluting the working solutions in complete medium to the desired concentration and used immediately for the cell treatments. In order to avoid any possible thawing/freezing-based degradation or moisture enrichment from the environment, the working solutions were prepared in different bulks for each compound, and were used only once.

4.2. NSRE modulation measured by means of gene reporter assays

The biological assay made use of the reporter cell line DiaNRSE^{LUC8}, which was originally derived by engineering ST14A neural progenitor cells with the RE1/NRSE^{BDNF}-LUC construct as previously described.[21] The DiaNRSE^{LUC8} cells were plated in white, clear-bottomed, 96-well plates (Corning Glasswork, Corning, NY, USA) (6000 cells/well) and, in parallel, in clear 96-well plates (Iwaki) in a final volume of 100 μl of complete medium.[21] After adhesion, the cells were exposed to 50 nM of the different compounds for 72 h in triplicate experiments, and then the white plates were used to evaluate luciferase activity (beetle luciferin, Promega Corp., Milano, Italy) and the clear plates to assess cell viability (MTT assay, SIGMA, Milano, Italy), as previously described.[21] The luminescent signals were measured using a VICTOR3 plate reader (PerkinElmer, Milano, Italy): a total of 45 readings were collected at 1-second intervals under each condition, and the kinetic average of the signals and related standard deviations and % coefficient of variation (CV) were analysed using WorkOut 2.0 software. Cell viability was assessed by reading absorbance at 560 nm using the VICTOR3 plate reader.

The results for each experimental condition are expressed as counts per second (CPS)/% of live cells in the treated versus the untreated control sample. Each test plate included cells treated with 75 nM of TSA (positive control) or DMSO only (untreated control).

4.3. Molecular modelling and 3D-QSAR

Forty-two derivatives (see Table S2, Supporting Information) were selected as a QSAR data-set, and Phase version 2.0.212 was used for pharmacophore elucidation and QSAR model building.[22] All the ligands were processed using the LigPrep program to assign protonation states appropriate for pH 7, using the 'ioniser' subprogram,[26] and conformers were generated using the MacroModel ligand torsion search (MMFF94s force field) and default parameters.[27,28] With activity defined as $[\log(FI)] \times 100$, the active ligands were defined as those with a $[\log(FI)] \times 100$ value of >18, and the inactive ligands as those with a $[\log(FI)] \times 100$ value of <18. Hypotheses were generated by systematically varying the number of sites (n_{sites}) and the number of matching active compounds (n_{act}). With $n_{act} = n_{act\_tot}$ initially (n_{act_tot} is the total number of active compounds in the training set), n_{sites} was varied from 7 to 3 until at least one hypothesis was found and scored successfully; if this failed, n_{act} was decreased by one and the n_{sites} cycle was repeated. The hypotheses were scored and weighted to include the consideration of the alignment of inactive compounds using default parameters. All the hypotheses successfully generated and scored in this manner were then used to build atom-based 3D-QSAR models with 1–3 partial-least-square factors. The statistics concerning the between predicted with actual activity were collated for the top ten scoring hypotheses using the default hypothesis scoring functions.

Acknowledgements

We thank the Ministry for University and Research (MiUR), Rome, Italy, for its financial support. Samantha Leone is supported by 'Sovvenzione Globale INGENIO: Fondo Sociale Europeo, Ministero del Lavoro e della Previdenza Sociale, Regione Lombardia', Protocol No. A0000170. We gratefully acknowledge STEM HD FP6 LSH-2005-1.2.4-5 Contract No. 037349 to Dialectica. The 3D-QSAR study coordinated by Stefano Moro was carried out with the financial support of the University of Padua, Italy and the MiUR; Stefano Moro is also very grateful to Schrödinger and Chemical Computing Group for their scientific and technical partnerships.

Supplementary data

Extended tables with activities and structures of the 84 tested compounds (Table S1), and training and test sets used for 3D-QSAR (Table S2). Supplementary data associated with this article can be found, in the online version, at doi:10.1016/j.bmc.2008.03.067.

References and notes

1. Hersch, S. M. *Curr. Opin. Neurol.* **2003**, *16*, 501.
2. Ryu, H.; Ferrante, R. J. *Expert Opin. Emerg. Drugs* **2005**, *10*, 345.
3. Di Prospero, N. A.; Fischbeck, K. H. *Nat. Rev. Genet.* **2005**, *6*, 756.
4. Cattaneo, E.; Zuccato, C.; Tartari, M. *Nat. Rev. Neurosci.* **2005**, *6*, 919.
5. Sipione, S.; Cattaneo, E. *Mol. Neurobiol.* **2001**, *23*, 21.
6. Roopra, A.; Sharling, L.; Wood, I. C.; Briggs, T.; Bachfischer, U.; Paquette, A. J.; Buckley, N. J. *Mol. Cell. Biol.* **2000**, *20*, 2147.
7. Bruce, A. W.; Donaldson, I. J.; Wood, I. C.; Yerbury, S. A.; Sadowski, M. I.; Chapman, M.; Gottgens, B.; Buckley, N. J. *Proc. Natl. Acad. Sci. U.S.A.* **2004**, *101*, 10458.
8. Johnson, R.; Gamblin, R. J.; Ooi, L.; Bruce, A. W.; Donaldson, I. J.; Westhead, D. R.; Wood, I. C.; Jackson, R. M.; Buckley, N. J. *Nucleic Acids Res.* **2006**, *34*, 3862.
9. Ooi, L.; Wood, I. C. *Nat. Rev. Genet.* **2007**, *8*, 544.
10. Timmusk, T.; Palm, K.; Lendhal, U.; Metsis, M. *J. Biol. Chem.* **1999**, *274*, 1078.
11. Zuccato, C.; Cattaneo, E. *Prog. Neurobiol.* **2007**, *81*, 294.
12. Wood, I. C.; Belyaev, N. D.; Bruce, A. W.; Jones, C.; Mistry, M.; Roopra, A.; Buckley, N. J. *J. Mol. Biol.* **2003**, *334*, 863.
13. Zuccato, C.; Ciammola, A.; Rigamonti, D.; Leavitt, B. R.; Goffredo, D.; Conti, L.; MacDonald, M. E.; Friedlander, R. M.; Silani, V.; Hayden, M. R.; Timmusk, T.; Sipione, S.; Cattaneo, E. *Science* **2001**, *293*, 493.
14. Zuccato, C.; Tartari, M.; Crotti, A.; Goffredo, D.; Valenza, M.; Conti, L.; Cataudella, T.; Leavitt, B. R.; Hayden, M. R.; Timmusk, T.; Rigamonti, D.; Cattaneo, E. *Nat. Genet.* **2003**, *35*, 76.
15. Zuccato, C.; Belyaev, N.; Conforti, P.; Ooi, L.; Tartari, M.; Papadimou, E.; MacDonald, M.; Fossale, E.; Zeitlin, S.; Buckley, N. J.; Cattaneo, E. *J. Neurosci.* **2007**, *27*, 6972.
16. Zuccato, C.; Tartari, M.; Goffredo, D.; Cattaneo, E.; Rigamonti, D. *Pharmacol. Res.* **2005**, *52*, 245.
17. Palm, K.; Belluardo, N.; Metsis, M.; Timmusk, T. *J. Neurosci.* **1998**, *18*, 1280.
18. Calderone, A.; Jover, T.; Noh, K. M.; Tanaka, H.; Yokota, H.; Lin, Y.; Grooms, S. Y.; Regis, R.; Bennet, M. V.; Zukin, R. S. *J. Neurosci.* **2003**, *23*, 2112.
19. Bahn, S.; Mimmack, M.; Ryan, M.; Caldwell, M. A.; Jauniaux, E.; Starkey, M.; Svendsen, C. N.; Emson, P. *Lancet* **2002**, *359*, 310.
20. Lawinger, P.; Venugopal, R.; Guo, Z. S.; Immaneni, A.; Sengupta, D.; Lu, W.; Rastelli, L.; Marin Dias Carneiro, A.; Levin, V.; Fuller, G. N.; Echelard, Y.; Majumder, S. *Nat. Med.* **2000**, *6*, 826.
21. Rigamonti, D.; Bolognini, D.; Mutti, C.; Zuccato, C.; Tartari, M.; Sola, F.; Valenza, M.; Kazantsev, A. G.; Cattaneo, E. *J. Biol. Chem.* **2007**, *282*, 24554.
22. *Phase*, version 2.0.212; Schrödinger, LLC: New York, 2005.
23. Dixon, S. L.; Smondyrev, A. M.; Knoll, E. H.; Rao, S. N.; Shaw, D. E.; Friesner, R. A. *J. Comput-Aided Mol. Des.* **2006**, *20*, 647.
24. von Grotthuss, M.; Pas, J.; Rychlewski, L. *Bioinformatics* **2003**, *19*, 1041.
25. Daylight Chemical Information Systems, **2000**, http://daylight.com.
26. LigPrep, version 2.1; Schrödinger, LLC: New York, 2005.
27. MacroModel, version 9.5; Schrödinger, LLC: New York, 2005.
28. Halgren, T. A. *J. Comput. Chem.* **1999**, *20*, 720.